

# Molecular Multistate Systems Formed in Two-Dimensional Porous Networks on Ag(111)

Kyung-Hoon Chung,<sup>†</sup> Howon Kim,<sup>†</sup> Won Jun Jang,<sup>†</sup> Jong Keon Yoon,<sup>†</sup> Se-Jong Kahng,<sup>\*,†</sup> Jinhwan Lee,<sup>\*,‡</sup> and Seungwu Han<sup>§</sup>

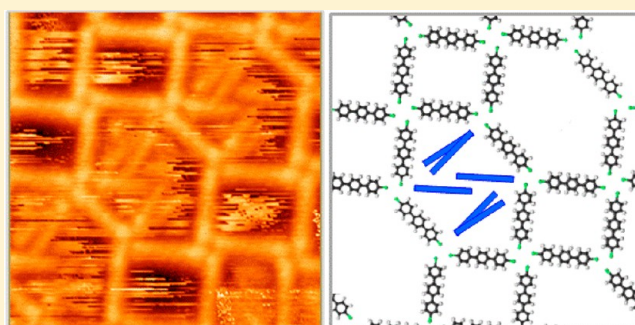
<sup>†</sup>Department of Physics, Korea University, 1-5 Anam-dong, Seongbuk-gu, Seoul 136-713, Republic of Korea

<sup>‡</sup>Department of Physics, KAIST, Daejeon 305-701, Republic of Korea

<sup>§</sup>Department of Materials Science and Engineering, Seoul National University, Seoul 151-744, Republic of Korea

## S Supporting Information

**ABSTRACT:** Host–guest interactions in porous supramolecular structures have been studied on surfaces using scanning tunneling microscopy, with anticipation of biochemical and sensor applications, but limited to cases of van der Waals interactions and hydrogen bonds. Here, we studied the intermolecular structures of 4,4''-dibromo-*p*-terphenyl molecules self-caged in porous supramolecular structures with halogen bonds on Ag(111). The caged molecules hopped among six different configurations at higher than 50 K, showing a propeller-like pattern. At 30 K, they stayed at one of six states that were stabilized with Br⋯Br halogen bonds and Br⋯H hydrogen bonds with energy gains of 225, 197, and 163 meV, as revealed by our density functional theory calculations. The self-caged structure provides a model system to simulate multistate supramolecular memories.



The self-caged structure provides a model system to simulate multistate supramolecular memories.

Supramolecular porous structures have been actively studied due to their possible applications in biochemical devices.<sup>1,2</sup> They are fabricated by self-assembly processes that are driven by molecule–molecule interactions. The forms of various two-dimensional (2d) porous structures have been revealed on crystal surfaces using scanning tunneling microscopy (STM).<sup>3–10</sup> The two-dimensional porous structures were used as molecular templates (host) to confine the second molecules (guest) in their periodic voids, and the interactions between host–guest molecules were examined due to their potential applications in conformational switching and chemical sensing.<sup>11–14</sup> C<sub>60</sub> molecules were trapped in the hexagonal voids made by perylene tetracarboxylic diimide and melamine on Ag/Si(111).<sup>11</sup> Phthalocyanine or coronene molecules were placed into the tetragonal voids of 1,3,5-tris(10-carboxydecyloxy) benzene on a graphite surface.<sup>12</sup> Porphyrin molecules have been nested on top of voids of 3,5-di(*tert*-butyl)phenyl in six equivalent directions on Cu(111).<sup>13</sup> Sexiphenyl-based long molecules were self-caged into honeycomb voids on Ag(111).<sup>14</sup> The rotation of a guest molecule has been observed in the porphyrin system, and switching between two rotational states has been observed in the sexiiphenyl-based system.<sup>13,14</sup> In these examples, the binding mechanisms between host and guest molecules were limited to van der Waals interactions and hydrogen bonds.

In this study, we report on the host–guest interactions in the self-caging system of 4,4''-dibromo-*p*-terphenyl (DBTP) molecules, with halogen bonds on Ag(111) using STM. A

rod-like DBTP molecule was caged in a hexagonal void and hopped among six stable configurations showing propeller-like patterns in the STM images above 50 K. The six configurations were stabilized by two interactions, Br⋯Br halogen bonds and Br⋯H hydrogen bonds.<sup>15–24</sup>

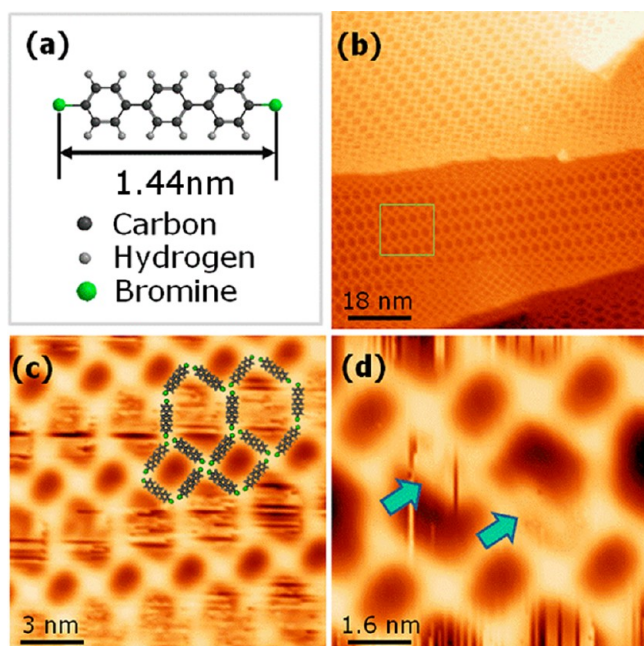
## RESULTS AND DISCUSSION

Figure 1a shows the DBTP molecule structure of three phenyl rings and two Br terminations. The molecules had large enough surface diffusivity to form self-assembled network structures when DBTP was deposited at 150 K. After deposition, the sample was cooled to 80 K to perform the STM measurement, and a typical STM image obtained from DBTP on Ag(111) is shown in Figure 1b. The DBTP molecules formed porous two-dimensional structures consisting of alternating rows of rectangles and hexagons, which covered ~70% of the surface. The hexagon had two 90° angles and four 135° angles. The 90° angles formed when four molecules make a quartet node, whereas the 135° angles formed when three molecules make a triple node. Each node possessed chirality. Namely, quartet nodes were clockwise, whereas triple nodes were anticlockwise in Figure 1. The mirror structures in Figure 1 made of anticlockwise quartet and clockwise triple nodes were also

Received: September 26, 2012

Revised: December 3, 2012

Published: December 11, 2012



**Figure 1.** (a) Chemical structure of the 4,4'-dibromo-*p*-terphenyl (DBTP) molecule. (b) A typical scanning tunneling microscopy (STM) topography image of porous networks obtained after a DBTP molecule was deposited on Ag(111) at 150 K. (c) A zoomed image from the square marked areas of panel b, which is superimposed with molecular models. The hexagonal voids were fuzzy or noisy, whereas the rectangular voids were clean. (d) A STM image obtained after hexagonal structures were disrupted by the STM tip. Caged molecules are identified in the image. Sizes of STM images: (b)  $90 \times 90 \text{ nm}^2$ , (c)  $15 \times 15 \text{ nm}^2$ , and (d)  $8 \times 8 \text{ nm}^2$ . Sample voltages: (b,c)  $V_S = 1 \text{ V}$  and (d)  $V_S = 0.8 \text{ V}$ . Tunneling current:  $I_T = 0.1 \text{ nA}$  for all images.

observed in our sample (see Figure 1S, Supporting Information). In Figure 1c, the inner parts of hexagons were fuzzily or noisily imaged, whereas those of rectangles were clearly imaged with no fuzziness. This behavior is explained by the scenario that a DBTP molecule is engaged in a hexagonal void and keeps moving due to thermal excitation. Rectangles may not have large enough voids ( $3.5 \text{ nm}^2$ ) to encage a DBTP molecule compared to hexagons ( $8.4 \text{ nm}^2$ ). When the structure of a hexagon was accidentally disrupted by a STM tip, the caged molecule stopped moving and was identified in the subsequent STM image in Figure 1d.

Instead of fuzziness, we sometimes observed a regular propeller-like pattern in the hexagonal voids, as shown in Figure 2a. The propeller comprised four blades, suggesting that a caged DBTP molecule hopped around four stable adsorption configurations permitted by the hexagon structure. We propose four different adsorption configurations, C1–C4, as they were superimposed over the propeller-like patterns of the STM images in Figure 2b. (Similar modeling is shown in Figure 1S, Supporting Information, and Figure 6b). We confirmed that the hexagon structures formed without a caged molecule and that there was no noticeable difference between hexagons with and without a caged molecule. Therefore, molecules that arrive at the surface after forming the hexagon structures must be engaged.

The structures of a hexagon and a caged molecule were superimposed with simplified electrostatic potential distributions in Figure 3 to identify possible intermolecular bonds.<sup>24</sup> Br atoms have both positive and negative potential regions with

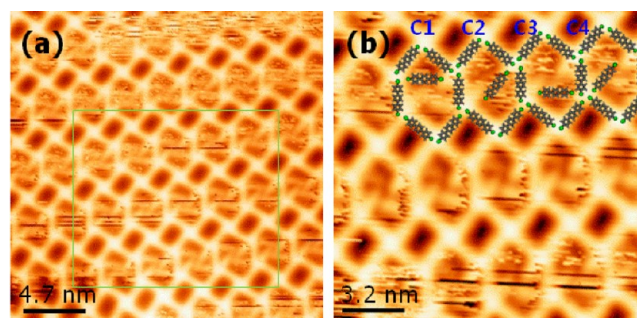


**Figure 2.** (a) Scanning tunneling microscopy (STM) topography images of hexagonal and rectangular networks with a regular propeller-like pattern inside the hexagons. (b) High-resolution STM images (a). Molecular models are superimposed over the image with six different configurations, C1–C4. Sizes of STM images: (a)  $23.5 \times 23.5 \text{ nm}^2$  and (b)  $16 \times 16 \text{ nm}^2$ . Sample voltages: (a)  $V_S = 1 \text{ V}$  and (b)  $V_S = 1.5 \text{ V}$ . Tunneling current,  $I_T = 0.1 \text{ nA}$  for all images.

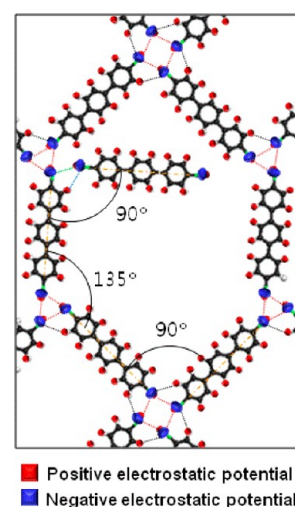


**Figure 3.** Molecular model with simplified electrostatic potential distributions overlaid on the hexagon structures with a caged molecule. Positive and negative potential distributions are represented with red and blue colors, respectively. Br has unique potential distribution with both the positive and negative potentials. Dotted lines indicate possible intermolecular bonds, Br...Br (red and green) and Br...H (black and blue).

cylindrical symmetry about the covalent bond axis, providing the origin of halogen bonds.<sup>19,24</sup> When there is no caged molecule, a hexagon is made of six DBTP molecules connected with 6 Br...Br halogen bonds and two Br...H hydrogen bonds, denoted with red and black dotted lines, respectively, in Figure 3. At a  $135^\circ$  angle, a Br...Br halogen bond forms, and at a  $90^\circ$  angle, a similar Br...Br halogen bond and an additional Br...H hydrogen bond form.<sup>24</sup> When a DBTP molecule is caged in a hexagon, the caged molecule may adhere to an existing  $135^\circ$  angle at a triple node, splitting the  $135^\circ$  angle into  $90^\circ$  and  $45^\circ$  angles. This suggests that the caged molecule may be stabilized by forming a  $90^\circ$  angle, with a Br...Br and a Br...H bond as depicted with the green and blue dotted lines, respectively, in Figure 3.

We performed density functional theory (DFT) calculations to investigate the detailed arrangement of caged molecules in the hexagon structures. We realized that the four corners of  $135^\circ$  angles in a hexagon could be classified into two, due to the detailed symmetry of nodes. The C1 and C3 configurations in

Figure 2b formed type A corners, which had two stable configurations, A1 and A2, as shown in Figure 4. The C2 and

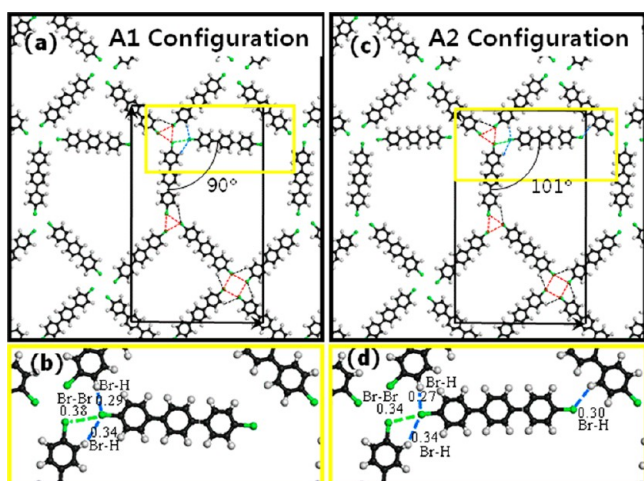


**Figure 4.** Atomic structure of (a) A1 configuration and (c) A2 configuration obtained from the density functional theory (DFT) calculations. The unit cell is drawn with black solid lines. Dotted lines indicate possible intermolecular bonds, Br $\cdots$ Br (red and green) and Br $\cdots$ H (black and blue). A zoom-in of the region marked with yellow lines (b) in panel a and (d) in panel c. The distances of possible intermolecular bonds are presented in nanometers.

C4 configurations in Figure 2b formed type B corners, which had one stable configuration B1, as shown in Figure 5. Therefore, we found six stable configurations for a caged molecule in the hexagon. In both the A1 and B1 configurations, a caged molecule split the 135° angle into 90° and 45° angles, as shown in Figures 4a and 5a. A caged molecule split a 135° angle into 101° and 34° angles in the A2 configuration of Figure 4c. Both the A1 and B1 configurations had three intermolecular bonds, whereas the A2 configuration had four intermolecular bonds. In the A1 configuration, the distances of Br $\cdots$ Br and two Br $\cdots$ Hs were 0.38, 0.29, and 0.34 nm, respectively, as shown in Figure 4b. In the B1 configuration, the distances of Br $\cdots$ Br and two Br $\cdots$ H were 0.37, 0.30, and 0.31 nm, respectively, as shown in Figure 5b. In the A2 configuration, the distances of Br $\cdots$ Br and three Br $\cdots$ Hs were 0.34, 0.27, 0.34, and 0.30 nm, respectively. Because these distances were similar to the sum of van der Waals radii for a Br $\cdots$ Br (0.38 nm) and a Br $\cdots$ H (0.31 nm), a Br $\cdots$ Br halogen bond and two Br $\cdots$ H hydrogen bonds were the real entities stabilizing the caged molecules. The additional energy gain produced by the interaction between a hexagon structure and a caged molecule was extracted by comparing the total energies of a hexagon structure with and without a caged molecule. The additional energy gains were 197, 225, and 163 meV for the A1, A2, and B1 configurations, respectively, showing reasonable agreement with the estimated bond energies of Br $\cdots$ Br (60 meV) and Br $\cdots$ H (70 meV).<sup>23–28</sup> Therefore, the results clearly show that a caged molecule was stabilized with Br $\cdots$ Br halogen bonds and Br $\cdots$ H hydrogen bonds. We found another stable structure at the type B corner, as described in Supporting Information. This structure did not match our experimental results and may not form, possibly due to a substrate or kinetic effect.

We expected four stable configurations based on our experimental results in Figures 1 and 2. However, the DFT

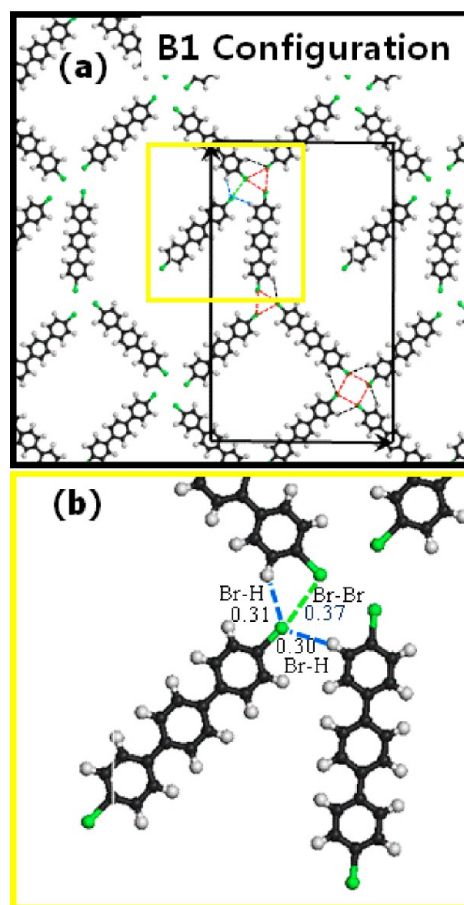


**Figure 5.** (a) Atomic structure of the B1 configuration obtained from density functional theory (DFT) calculations. The unit cell is drawn with gray solid lines. Dotted lines indicate possible intermolecular bonds, Br $\cdots$ Br (red and pink) and Br $\cdots$ H (black and blue). (b) A zoom-in of the region marked with yellow lines in panel a. The distances of possible intermolecular bonds are presented in nanometers.

calculations yielded six stable configurations. Thus, we performed STM experiments at lower temperatures. At 30 K, caged molecules were fixed to one of the four 135° corners of the hexagon. Figure 6a shows two caged molecules that are

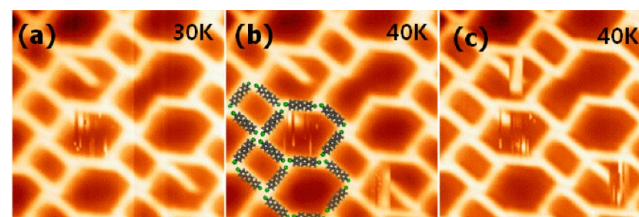


**Figure 6.** (a–c) Series of scanning tunneling microscopy (STM) topography images obtained at (a) 30 K and (b,c) 40 K, with a few caged molecules. Sizes of STM images: 12 × 12 nm<sup>2</sup>. Tunneling current,  $I_T = 0.1$  nA, and sample voltage,  $V_S = 0.6$  V, for all images.

fixed in the B1 configuration of the hexagon. Because of different coverage between Figures 6a and 2a, only two caged molecules are shown in Figure 6a. Caged molecules began to hop between neighboring configurations at 40 K. One caged molecule stayed fixed to the B1 configuration, whereas the other caged molecule switched between B1 and A1

configurations (Figure 6b). Both caged molecules switch in Figure 6c. We observed that the caged molecule in the A1 configuration was fuzzy compared to the molecule at B2, suggesting that the molecule in the A1 configuration actually switched between A1 and A2 and did not stay at one of the two configurations. Caged molecules actively hopped among six stable configurations at 50 K. The STM images in Figure 7a,b

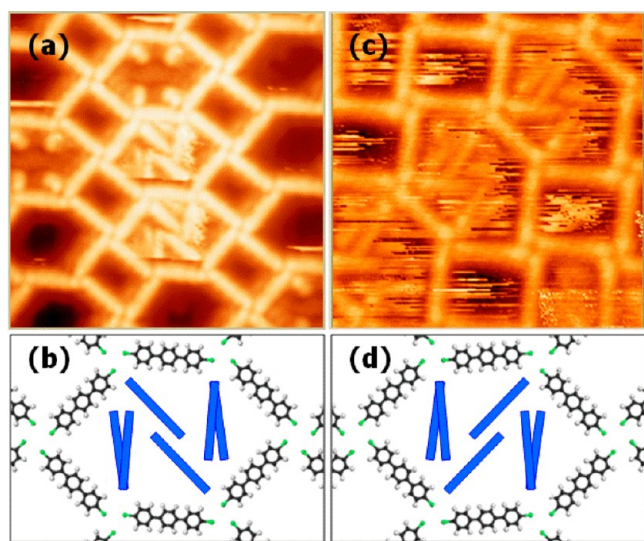


**Figure 7.** (a,c) Scanning tunneling microscopy (STM) topography images obtained at 50 K. The windmill-like nodes in panels a and c possess opposite chirality. (b,d) Molecular structure of a caged molecule in panels a and c, respectively. The caged molecule is depicted with a bar for simplicity.

clearly show that the caged molecules had six stable configurations, as schematically depicted in Figure 7b,d). It should be noted that the two hexagon structures in Figure 7a,b showed opposite chirality and that their structure could be explained by the six configurations discussed above. In Figures 6 and 7, shorter molecules were encaged in hexagons than DBAQ. They seem to be dibromobenzene (DBB) molecules, which were used in the DBAQ synthesis. They may have been unfiltered during the purification process. As the DBB molecules also have two Br ligands, they take similar binding configurations as those of DBAQ, by means of Br–Br and Br–H bonds.

## CONCLUSIONS

We studied a self-caged molecular structure in DBTP on Ag(111) using STM. The caged molecule had six stable configurations in a hexagonal structure. At higher than 50 K, the caged molecule hopped among six states to form a propeller-like pattern. The six states were stabilized with Br⋯Br halogen bonds and two Br⋯H hydrogen bonds. This system can work as a model system for a supramolecular memory array. A caged molecule can be switched from one state to another through STM manipulation techniques. However, it is challenging to induce switching between two randomly chosen states selectively.

## EXPERIMENTAL SECTION

STM experiments were performed using a home-built STM housed in an ultrahigh vacuum (UHV) chamber with a base pressure of  $<7 \times 10^{-11}$  Torr. An Ag(111) single crystal was

cleaned by several cycles of Ne-ion sputtering and annealing at 800 K. Commercially available DBTP (Tokyo Chemical Industry, Tokyo, Japan) was thermally evaporated on the Ag(111) surface at submonolayer coverage from an alumina-coated crucible, keeping the substrate temperature at 150 K. The DBTP molecules were outgassed for several hours prior to deposition. The molecular flux was about  $0.1/\text{nm}^2 \cdot \text{min}$ . The prepared sample was transferred to the STM and cooled down to 30–80 K. A Pt–Rh alloy tip was used as the STM probe.

## THEORETICAL CALCULATIONS

We performed first-principles density functional calculations using the VASP code.<sup>29,30</sup> Interaction between ions and electrons was approximated by the projector-augmented wave potential.<sup>31</sup> A generalized gradient approximation (with the Perdew–Burke–Ernzerhof (PBE) function) was used to describe the exchange correlations between electrons.<sup>32</sup> The energy cutoff for the plane wave basis was set to 500 eV. The lattice parameters and molecular geometries were very similar to those based on the PBE function. To describe nonbonding interactions between the molecules, particularly of the van der Waals type, an empirical correction scheme proposed by Grimme et al. was adopted.<sup>33</sup> The energy for an isolated molecule was obtained using a  $25 \times 15 \times 10 \text{ \AA}^3$  supercell. A simulation cell containing five DBTP molecules for porous structures and a DBTP molecule for the guest was used to describe the periodic structure. The height of the simulation box perpendicular to the molecule plane was fixed at 10 Å, whereas the lateral parameters were optimized such that the residual stress was  $<1$  kbar. We first found the optimized configurations of the hexagonal porous structures and then introduced a guest molecule to determine the stable adsorption configurations. For initial conditions, the center of molecule was located at various sites within the area of  $0.3 \times 0.3 \text{ nm}^2$  and at various angles within a  $60^\circ$  span, around the relaxed configuration.

## ASSOCIATED CONTENT

### Supporting Information

Chirality of nodes and configurations. This material is available free of charge via the Internet at <http://pubs.acs.org>.

## AUTHOR INFORMATION

### Corresponding Author

\*Tel: (+82) 2-3290-3109. Fax: (+82) 2-922-3484. E-mail: [sjkahng@korea.ac.kr](mailto:sjkahng@korea.ac.kr) (S.-J.K.); [jhinwan@kaist.ac.kr](mailto:jhinwan@kaist.ac.kr) (J.L.).

### Notes

The authors declare no competing financial interest.

## ACKNOWLEDGMENTS

We gratefully acknowledge financial support from the Ministry of Education Science and Technology of the Korean government through the National Research Foundation (2010-0025301 and 2012-0013222). S.H. was supported by the Center for Multiscale Energy System. This study was supported by the Supercomputing Center/Korea Institute of Science and Technology Information with supercomputing resources including technical support (KSC-2012-C1-10).

## REFERENCES

(1) Wehrspohn, R. B., Ed. *Ordered Porous Nanostructures and Applications*; Springer: New York, 2011.

- (2) Rao, C. N. R.; Natarajan, S.; Vaidhyanathan, R. *Angew. Chem., Int. Ed.* **2004**, *43*, 1466–1496.
- (3) Elemans, J. A. A. W.; Lei, S.; Feyter, S. D. *Angew. Chem., Int. Ed.* **2009**, *48*, 7298–7332.
- (4) Barth, J. V.; Costantini, G.; Kern, K. *Nature* **2005**, *437* (29), 671–679.
- (5) Kudernac, T.; Lei, S.; Elemans, J. A. A. W.; Feyter, S. D. *Chem. Soc. Rev.* **2009**, *38*, 402–421.
- (6) Tait, S. L.; Langner, A.; Lin, N.; Chandrasekar, R.; Fuhr, O.; Ruben, M.; Kern, K. *ChemPhysChem* **2008**, *9*, 2495–2499.
- (7) Stepanow, S.; Lingensfelder, M.; Dmitriev, A.; Spillmann, H.; Delvigne, E.; Lin, N.; Deng, X.; Cai, C.; Barth, J. V.; Kern, K. *Nature* **2004**, *3*, 229–233.
- (8) Pawin, G.; Wong, K. L.; Kwon, K.-Y.; Bartels, L. *Science* **2006**, *313*, 961–962.
- (9) Klappenberger, F.; Kühne, D.; Krenner, W.; Silanes, I.; Arnau, A.; de Abajo, F. J. G.; Klyatskaya, S.; Ruben, M.; Barth, J. V. *Nano Lett.* **2009**, *9* (10), 3509–3514.
- (10) Schlick, U.; Decker, R.; Klappenberger, F.; Zoppellaro, G.; Klyatskaya, S.; Auwarter, W.; Neppel, S.; Kern, K.; Brune, H.; Ruben, M.; Barth, J. V. *J. Am. Chem. Soc.* **2008**, *130*, 11778–11782.
- (11) Theobald, J. A.; Oxtoby, N. S.; Phillips, M. A.; Champness, N. R.; Beton, P. H. *Nature* **2003**, *424*, 1029.
- (12) Lu, J.; Lei, S. B.; Zeng, Q. D.; Kang, S. Z.; Wang, C.; Wan, L. J.; Bai, C. L. *J. Phys. Chem. B* **2004**, *108*, 5161.
- (13) Wintjes, N.; Bonifazi, D.; Cheng, F.; Kiebele, A.; Stöhr, M.; Jung, T.; Spillmann, H.; Diederich, F. *Angew. Chem., Int. Ed.* **2007**, *46*, 4089.
- (14) Kühne, D.; Klappenberger, F.; Krenner, W.; Klyatskaya, S.; Ruben, M.; Barth, J. V. *Proc. Natl. Acad. Sci.* **2010**, *107*, 21332–21336.
- (15) Mentrangolo, P.; Meyer, F.; Pilati, T.; Resnati, G.; Terraneo, G. *Angew. Chem., Int. Ed.* **2008**, *47*, 6114–6127.
- (16) Desiraju, G. R.; Parthasarathy, R. *J. Am. Chem. Soc.* **1989**, *111*, 8725–8726.
- (17) Aakeröy, C. B.; Fasulo, M.; Schultheiss, N.; Desper, J.; Moore, C. J. *J. Am. Chem. Soc.* **2007**, *129*, 13772–13773.
- (18) Walch, H.; Gutzler, R.; Sirtl, T.; Eder, G.; Lackinger, M. *J. Phys. Chem. C* **2010**, *114*, 12604–12609.
- (19) Yoon, J. K.; Son, W.-J.; Chung, K.-H.; Kim, H.; Han, S.; Kahng, S.-J. *J. Phys. Chem. C* **2011**, *115*, 2297–2301.
- (20) Yoon, J. K.; Son, W.-J.; Kim, H.; Chung, K.-H.; Han, S.; Kahng, S.-J. *Nanotechnology* **2011**, *22*, 275705.
- (21) Russell, J. C.; Blunt, M. O.; Garfitt, J. M.; Scurr, D. J.; Alexander, M.; Champness, N. R.; Beton, P. H. *J. Am. Chem. Soc.* **2011**, *133*, 4220–4223.
- (22) Gutzler, R.; Ivasenko, O.; Fu, C.; Brusso, J. L.; Rosei, F.; Perepichka, D. F. *Chem. Commun.* **2011**, *47*, 9453–9455.
- (23) Park, J.; Kim, K. Y.; Chung, K.-H.; Yoon, J. K.; Kim, H.; Han, S.; Kahng, S.-J. *J. Phys. Chem. C* **2011**, *115*, 4834.
- (24) Chung, K.-H.; Park, J.; Kim, K. Y.; Yoon, J. K.; Kim, H.; Han, S.; Kahng, S.-J. *Chem. Commun.* **2011**, *47*, 11492.
- (25) Awwadi, F. F.; Willett, R. D.; Peterson, K. A.; Twamley, B. *Chem.—Eur. J.* **2006**, *12*, 8952–8960.
- (26) Kovács, A.; Varga, Z. *Coord. Chem. Rev.* **2006**, *250*, 710–727.
- (27) Futami, Y.; Kudoh, S.; Ito, F.; Nakanaga, T.; Nakata, M. *J. Mol. Struct.* **2004**, *690*, 9–16.
- (28) Xu, J.; Wang, W.-L.; Lin, T.; Sun, Z.; Lai, Y.-H. *Supramol. Chem.* **2008**, *20*, 723–730.
- (29) Kresse, G.; Hafner, J. *Phys. Rev. B* **1993**, *47*, 558–561.
- (30) Kresse, G.; Hafner, J. *Phys. Rev. B* **1994**, *49*, 14251–14269.
- (31) Blöchl, P. E. *Phys. Rev. B* **1994**, *50*, 17953–17979.
- (32) Perdew, J. P.; Burke, K.; Ernzerhof, M. *Phys. Rev. Lett.* **1996**, *77*, 3865–3868.
- (33) Grimme, S. *J. Comput. Chem.* **2004**, *25*, 1463–1473.